Appendix II

MACHINE SPECIFICATIONS

Rated speed, rpm	1800
Rated torque, Nm	3.96
Rated current, A	3
P, No. of pole pairs	2
R_s,R_c Ω	1.93, 330
L_d, L_q mH	42.44, 79.57
λ_m ,Wb	0.314
J, Rotorinertia constant, $Kg.m^2$	0.003
B, Viscous coefficient, Nm /rad /sec.	0.0008

Reference

[1] R. Schiferl, T.A. Lipo, "Power capability of salient pole permanent magnet synchronous motors in variable speed drive application", IEEE Trans. Ind. Appl., Vol.26, No.1, pp.115-123, Jan/Feb. 1990.

[2] K.J. Tseng, S.B. Wee, "Analysis of flux distribution and core losses in interior permanent magnet motor", IEEE Trans. on Ene. Conv., Vol.14, No.4, pp.969-975, Dec. 1999.

[3] S. Vaez-zadeh, M. Zamanifar, "Efficiency optimization control of IPM synchronous motor drives with on line parameter estimation", Jou. of Trans. on Elec. Tech. (JTET), Vol.1, No.4, pp.61-69, Aut. 2009.

[4] S. Vaez-Zadeh, S.M. Bakhtvar, "Cascade sliding mode control of permanent magnet synchronous motors", IEEE/IECON, Vol.3, pp.2051-2056, 2002.

[5] S. Morimoto, Y. Takeda, T. Hirasa, "Loss minimization control of permanent magnet synchronous motors", IEEE Trans. Ind. Elec., Vol.41, pp.511-517, Oct. 1994.

[6] D. Grenier, L. Dessaint, O. Akhrif, Y. Bonnassieux, B. Le Pioufle, "Experimental nonlinear torque control of a permanent magnet synchronous motor using saliency", IEEE Trans. on Ind. Elec., Vol.44, No.5, pp.680-687, Oct. 1997.

[7] C. Mademlis, I. Kioskeridis, N. Margaris, "Optimal efficiency control strategy for interior permanent-magnet synchronous motor drives", IEEE Trans. on Ene. Conv., Vol.19, No.4, pp.715-723, Dec. 2004.

[8] O. Ojo, F. Osaloni, Z. Wu, M. Omoigui, "A control strategy for optimum efficiency operation of high performance interior permanent magnet motor drives", IEEE/PESC, pp.604-610, Sep. 2003.

[9] T. Sebastian, "Temperature effects on torque production and efficiency of PM motors using NdFeB magnets", IEEE Trans. Ind. Appl., Vol.31, No.2, pp.353-357, Mar/Apr. 1995.

[10] S. Vaez-Zadeh, V.I. John, "Minimum loss operation of PM motor drives", IEEE/ECE, Vol.1, pp.284-287, Canada, Sep. 1995.

[11] S. Vaez-Zadeh, M.A. Rahman, "Energy saving vector control strategies for electric vehicle motor drives", IEEE/PCC, pp.13-18, 1997.

[12] V.I. Utkin, "Sliding mode control design principles and applications to electric drives", IEEE Trans. on Ind. Elec., Vol.40, No.1, pp.23-36, Feb. 1993.

[13] F.J. Lin, K.K. Shyu, Y.S. Lin, "Variable structure adaptive control for PM synchronous servo motor drives", IEE Proc. Elec. Pow. Appl., Vol.146, No.2, pp.173-185, Mar. 1999.

[14] F. Chen, M.W. Dunnigan, "Feedback linearization sliding mode torque control of an induction machine", IEEE/PEMD, pp.110-115, June 2002.

[15] K. Khalil Hassan, Nonlinear systems. 2nd ed. Upper Addle River, NJ: Prentice-hall, 1996.

The loss minimization control of IPM motor drives, introduced by Morimoto is simulated here for comparison [4]. Fig. (7) shows the speed response of both methods for two operating points. It can be seen that since the PI controllers of the Morimoto's method are tuned in nominal operating point, dynamics of other operating points are not desirable. But in the case of SMC, a change of operating point does not affect the desirable performance of the motor drive.

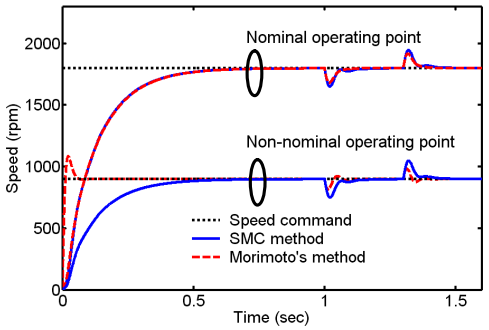

Fig. (10): Speed response of the proposed method and the Morimoto's method

In order to show the robustness of SMC against the parameter variations, another simulation is carried out where the motor parameters are assumed to vary over a certain pattern due to ambient and operating conditions. Efficiency and total electrical losses of the motor are shown in Figs. (11-12) for varying speed (at rated torque) and varying torque (at rated speed) respectively.

In these figures, three different pairs (η and P_{Loss}) of plots are shown. The first pair, shown by dash-doted line and used as a basis for comparison, is related to an ideal response of the controller in confronting to the parameter variations. It is obtained by assuming that the controller knows the exact value of the machine parameters which never happen in practice. The second pair of plot, shown by solid line, is the result of the SMC and the third one, shown by dashed line, is related to the method introduced by S. Morimoto. It can be seen that parameter variations have undesirable effect on the motor efficiency except in near the nominal operating conditions in both methods. However, it is seen that the SMC is more robust against parameter variations resulting in higher motor efficiency over a wide operating range.

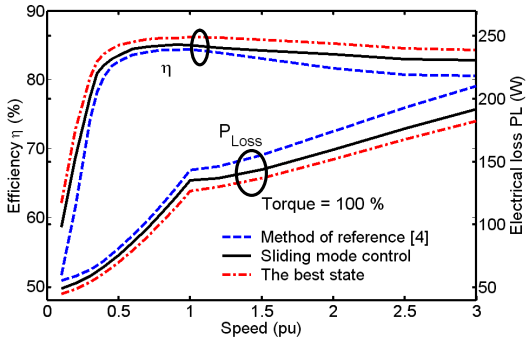

Fig. (11): Efficiency and electrical losses in terms of speed

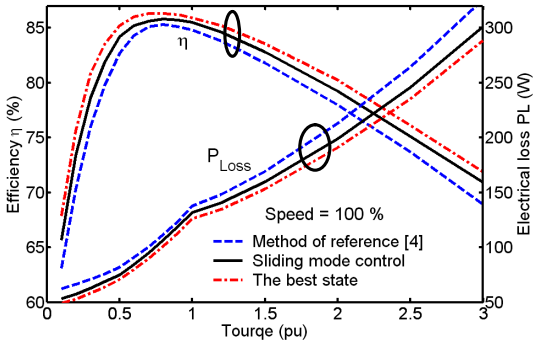

Fig. (12): Efficiency and electrical losses in terms of torque

VI. conclusion

In this paper, a high performance model-following nonlinear sliding mode controller based on a feedback linearization control system for an IPM synchronous motor has been described. This controller minimizes the motor losses besides the tracking of a reference speed. Moreover, the desirable robustness of the controlled IPM synchronous motor drive against the parametric uncertainties is improved resulting in a more energy saving over a wide motor operating range.

Appendix I

The matrix components of equation (13) are:

$$f_1 = \frac{3P}{2}\left\{\left(L_d - L_q\right)\omega_e\left(\frac{L_q}{L_d}i_{qT}^2 - \frac{L_d}{L_q}i_{dT}^2\right) + \frac{R_s R_c}{\left(R_s+R_c\right)}\frac{\left(L_q^2 - L_d^2\right)}{L_d L_q}i_{dT}i_{qT} + \frac{1}{L_q}\left(L_q - 2L_d\right)\lambda_m\omega_e i_{dT} - \frac{R_s R_c}{L_q\left(R_s+R_c\right)}\lambda_m i_{qT} - \frac{1}{L_q}\lambda_m^2\omega_e\right\} \tag{34}$$

$$f_2 = 2R_s\left(L_d - L_q\right)\left(\frac{R_s R_c}{L_d\left(R_s+R_c\right)} + \frac{L_d}{R_c}\omega_e^2\right)i_{dT}^2 - 2\frac{R_s^2 R_c\left(L_d - L_q\right)}{L_q\left(R_s+R_c\right)}i_{qT}^2 - 2\frac{2L_d L_q\omega_e^2}{R_c^2}\left(R_s+R_c\right)\left(L_d - L_q\right)\omega_e i_{dT}i_{qT} - 2\frac{R_s}{L_d L_q}\left(L_d^2 - L_q^2\right)\omega_e i_{dT}i_{qT}$$

$$- 2R_s\left(L_d - L_q\right)\frac{L_q}{R_c}\omega_e^2 i_{qT}^2 = \left(\frac{\omega_e^2}{R_c}\left(2L_d - L_q\right) + \frac{R_s R_c}{L_d\left(R_s+R_c\right)}\right)R_s\lambda_m i_{dT} - \frac{L_q\omega_e^2}{R_c^2}\left(R_s+R_s\right)\left(4L_d - 3L_q\right)\lambda_m\omega_e i_{qT} - \frac{R_s}{L_d L_q}\left(L_q^2 - 2L_d L_q + 2L_d^2\right)\lambda_m\omega_e i_{qT} \tag{35}$$

$$g_1 - \frac{3P}{2}\frac{R_c\left(L_d - L_q\right)}{L_d\left(R_s+R_c\right)}i_{qT} \tag{36}$$

$$g_2 = \frac{3P}{2}\frac{R_c}{L_q\left(R_s+R_c\right)}\left(\lambda_m + \left(L_d - L_q\right)i_{dT}\right) \tag{37}$$

$$g_3 = -2\left(L_d - L_q\right)\left(\frac{R_s R_c}{L_d\left(R_s+R_c\right)} + \frac{L_d}{R_c}\omega_e^2\right)i_{dT} - \frac{1}{R_c}\left(2L_d - L_q\right)\lambda_m\omega_e^2 - \frac{R_s R_c\lambda_m}{L_d\left(R_s+R_c\right)} \tag{38}$$

$$g_4 = 2\left(L_d - L_q\right)\left(\frac{R_s R_c}{L_q\left(R_s+R_c\right)} + \frac{L_q}{R_c}\omega_e^2\right)i_{qT} \tag{39}$$

V. Simulation Results

The performance of an IPM motor under the proposed model-following nonlinear sliding mode control system has been investigated by extensive simulation. The IPM synchronous motor specifications are listed in Appendix II. The overall motor drive block diagram is shown in Fig. (2). Many simulation runs have been carried out to examine the proposed SMC scheme. Firstly, an unloaded motor, T_L=0, is simulated. The motor is started by an exponential speed command reference with the final value of machine rated speed as in Fig. (3) Then at the time t=1 (sec) a rated load torque is applied to the motor. Reference Speed command is reduced exponentially to the half rated speed at t=1.5(sec). Subsequently, at t=2.5(sec) the rated load is removed from the motor.

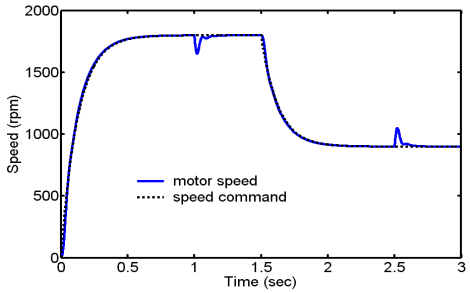

Fig. (3): Speed response

As it is expected, SMC rejects the external load disturbance. Also it can be seen that the chattering associated with the sliding mode exists with low amplitude in Fig. (4) which shows the load and the motor torque plots.

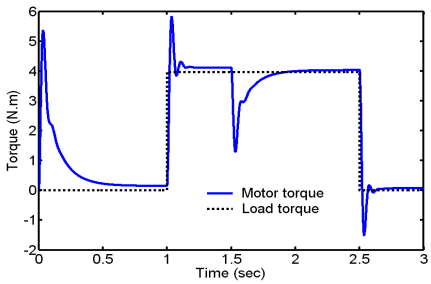

Fig. (4): Torque response

The d-q axis currents are also shown in Fig. (5). The simulation results confirm desirable motor performance under the proposed efficiency optimization controller.

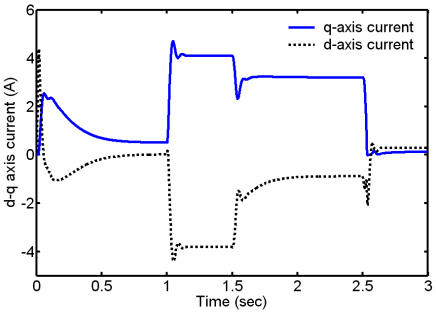

Fig. (5): d -q axis current response

Figs. (6-9) show the phase plot of the SMC. In Figs. (6) and (7) the two errors of e_1 and e_2 with respect to time are plotted. Also the effect of λ_1 and λ_2 values are shown in these figures. Sliding surfaces S_1 and S_2 are shown in Figs. (8) and (9). It is seen that the two errors oscillate and finally converge the zero point. This confirms the reachability of SMC the controlled system.

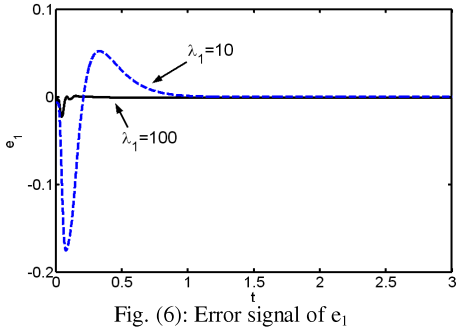

Fig. (6): Error signal of e_1

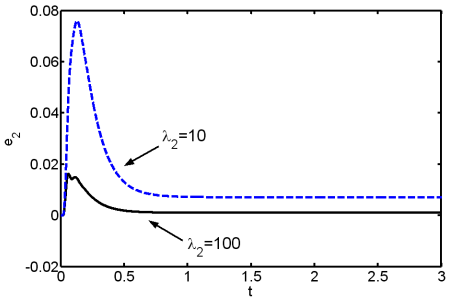

Fig. (7): Error signal of e_2

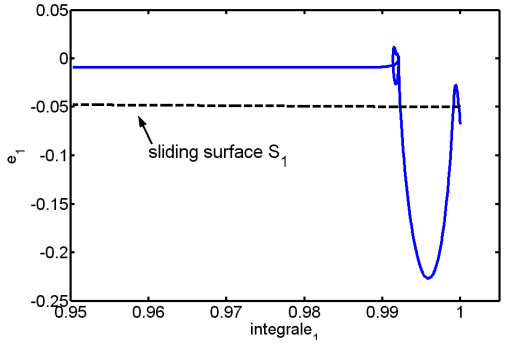

Fig. (8): Sliding surface of s_1

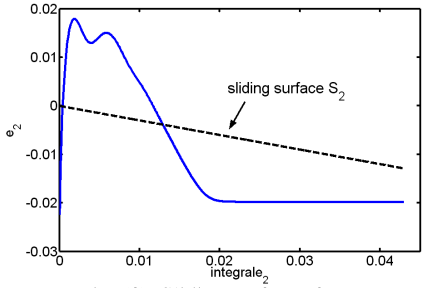

Fig. (9): Sliding surface of s_2

$$\begin{bmatrix}\dot{y}_{m1}\\ \dot{y}_{m2}\end{bmatrix}=\begin{bmatrix}-a_{m1} & 0\\ 0 & -a_{m2}\end{bmatrix}\begin{bmatrix}y_{m1}\\ y_{m2}\end{bmatrix}+\begin{bmatrix}a_{m1} & 0\\ 0 & a_{m2}\end{bmatrix}\begin{bmatrix}y_{1\_ref}\\ y_{2\_ref}\end{bmatrix} \quad (18)$$

where a_{m1} and a_{m2} are the designed positive constants with a_{m1} determining the reference torque performance and a_{m2} determining the reference loss minimization condition. Also we have:

$$y_{1\_ref}=T_{e\_ref}\ ,\ y_{2\_ref}=0 \quad (19)$$

The tracking errors between the plant of (16) and reference model are:

$$\begin{bmatrix}e_1\\ e_2\end{bmatrix}=\begin{bmatrix}y_1-y_{m1}\\ y_2-y_{m2}\end{bmatrix} \quad (20)$$

and its error dynamics are derived as follows:

$$\begin{bmatrix}\dot{e}_1\\ \dot{e}_2\end{bmatrix}=\begin{bmatrix}f_1\\ f_2\end{bmatrix}+\begin{bmatrix}0 & 1\\ 1 & 0\end{bmatrix}\begin{bmatrix}\nu'_d\\ \nu'_q\end{bmatrix}+\begin{bmatrix}\varphi_1\\ \varphi_2\end{bmatrix} \quad (21)$$

where φ_1 and φ_2 are assumed bounded parameter uncertainties and the linear feedback is:

$$\begin{bmatrix}\nu'_d\\ \nu'_q\end{bmatrix}=\begin{bmatrix}\hat{\nu}_d+a_{m2}y_{m2}-a_{m2}y_{2\_ref}\\ \hat{\nu}_q+a_{m1}y_{m1}-a_{m1}y_{1\_ref}\end{bmatrix} \quad (22)$$

Now, the sliding mode design technique can be used for the error system (21) to make the errors e_1 and e_2, reach zero. That is the developed torque and loss minimization condition track their reference values. The control algorithm consists of three steps:

- Calculating coordinate controller, ν'_d and ν'_q, according to the sliding mode method.
- Calculating $\hat{\nu}_d$ and $\hat{\nu}_q$ using feedback linearization control of (22).
- Calculating ν_d and ν_q using feedback linearization control of (16).

B. Sliding Mode Surface

In order that e_1 and e_2 converge to zero, two sliding surfaces are introduced as:

$$s_1=e_1+\lambda_1\int e_1.dt \quad (23)$$

$$s_2=e_2+\lambda_2\int e_2.dt \quad (24)$$

where the parameters λ_1 and λ_2 are positive constants which determine the convergence rate. A Lyapunov function is then proposed as:

$$V=\frac{1}{2}S_1^2+\frac{1}{2}S_2^2\ \Rightarrow \dot{V}=S_1\dot{S}_1+S_2\dot{S}_2 \quad (25)$$

By differentiating sliding surfaces and substituting from (22), we will have:

$$\dot{S}_1=f_1+\nu'_q+\varphi_1+\lambda_1e_1 \quad (26)$$

$$\dot{S}_2=f_2+\nu'_d+\varphi_2+\lambda_2e_2 \quad (27)$$

then:

$$\dot{V}=S_1\left[f_1+\nu'_q+\varphi_1+\lambda_1e_1\right]+S_2\left[f_2+\nu'_d+\varphi_2+\lambda_2e_2\right] \quad (28)$$

Assuming ν'_d and ν'_q as:

$$\nu'_d=-f_2-\lambda_2e_2-Q_2\,\mathrm{sgn}(S_2)\quad ,\ Q_2>\left|\varphi_2\right| \quad (29)$$

$$\nu'_q=-f_1-\lambda_1e_1-Q_1\,\mathrm{sgn}(S_1)\quad ,\ Q_1>\left|\varphi_1\right| \quad (30)$$

and substituting them in (28):

$$\begin{aligned}\dot{V}&=S_1\left[-Q_1\,\mathrm{sgn}(S_1)+\varphi_1\right]+S_2\left[-Q_2\,\mathrm{sgn}(S_2)+\varphi_2\right]\\ &\le\left|S_1\right|\left[-Q_1+\left|\varphi_1\right|\right]+\left|S_2\right|\left[-Q_2+\left|\varphi_2\right|\right]\le 0\end{aligned} \quad (31)$$

Hence, using the proposed controller (29) - (30), the reachability of sliding mode control of the controlled system (21) is guaranteed. After reaching the surfaces S_1 and S_2, the system output errors will converge to zero, that is:

$$y_1=T_e\rightarrow T_{e\_ref}\ ,\ y_2\rightarrow y_{2\_ref}=0 \quad (32)$$

The proposed sliding mode control is robust with respect to matched and mismatched uncertainties. In addition, with the use of the feedback linearization control, the complete decoupled control of torque and indirectly flux can be obtained.

The chattering associated with sliding mode is the main drawback of the sliding mode application. The sliding mode control chattering is substantially reduced if in equations (28) and (29), sgn (s_1) and sgn (s_2) are replaced by the following saturation function or by $\tan^{-1}$ function [15]:

$$\mathrm{Sat}\left(\frac{s}{\varphi}\right)=\begin{cases}+1 \text{ if} & s\succ\varphi\\ \dfrac{s}{\varphi} \text{ if} & -\varphi\le s\le\varphi\\ -1 \text{ if} & s\prec-\varphi\end{cases} \quad (33)$$

where ϕ is a positive parameter.

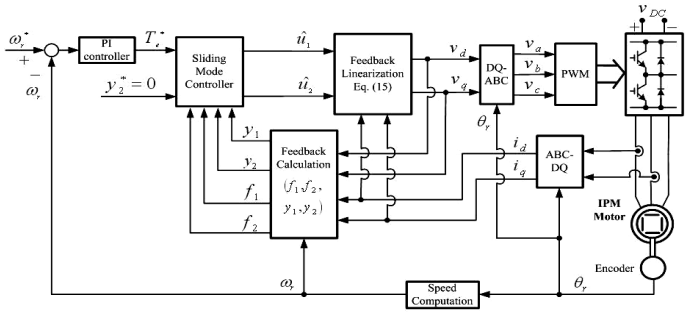

Fig. (2): IPM motor drive system block diagram

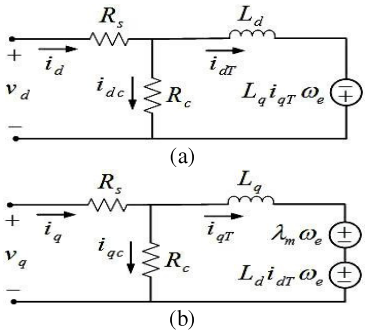

Fig. (1): Equivalent circuits for IPMS motor
(a) d axis. (b) q axis.

Conventional notation is used for machine parameters and variables. In steady state, the electrical power losses of the machine can be expressed as:

$$P_L = \frac{3}{2}R_s\left(i_{dT}^2 + i_{qT}^2\right) + 3\frac{\left(R_s + R_c\right)}{R_c^2}L_d\lambda_m\omega_e^2 i_{dT} + \frac{3}{2}\frac{\omega_e^2}{R_c^2}\left(R_s + R_c\right)\left(\lambda_m^2 + L_d^2 i_{dT}^2 + L_q^2 i_{qT}^2\right) + 3\frac{R_s}{R_c}\left(\lambda_m + \left(L_d - L_q\right)i_{dT}\right)\omega_e i_{qT} \quad (4)$$

III. Loss Minimization Condition

In this section, a loss minimization condition for an IPM synchronous motor is achieved. By differentiating (3) and (4) with respect to i_{dT} the following equations are obtained:

$$\frac{\partial T_e}{\partial i_{dT}} = \frac{3P}{2}\left[\lambda_m\frac{\partial i_{qT}}{\partial i_{dT}} + \left(L_d - L_q\right)\left(i_{qT} + i_{dT}\frac{\partial i_{qT}}{\partial i_{dT}}\right)\right] \quad (5)$$

$$\frac{\partial P_L}{\partial i_{dT}} = 3R_s\left(i_{dT} + \frac{\partial i_{qT}}{\partial i_{dT}}i_{qT}\right) + 3\frac{\left(R_s + R_c\right)}{R_c^2}L_d\lambda_m\omega_e^2 + 3\frac{R_s}{R_c}\left(\lambda_m\frac{\partial i_{qT}}{\partial i_{dT}} + \left(L_d - L_q\right)\left(i_{qT} + \frac{\partial i_{qT}}{\partial i_{dT}}i_{dT}\right)\right)\omega_e + 3\frac{\omega_e^2}{R_c^2}\left(R_s + R_c\right)\left(L_d^2 i_{dT} + L_q^2\frac{\partial i_{qT}}{\partial i_{dT}}i_{qT}\right) \quad (6)$$

In order to reach the loss minimization condition in every operating point, the above differentials must be equal to zero i.e.:

$$\frac{\partial T_e}{\partial i_{dT}} = 0\,,\ \frac{\partial P_L}{\partial i_{dT}} = 0 \quad (7)$$

then:

$$\frac{\partial i_{qT}}{\partial i_{dT}} = -\frac{\left(L_d - L_q\right)i_{qT}}{\lambda_m + \left(L_d - L_q\right)i_{dT}} \quad (8)$$

$$\frac{\partial i_{qT}}{\partial i_{dT}} = -\frac{P}{Q} \quad (9)$$

where:

$$P = R_s i_{dT} + \frac{R_s}{R_c}\left(L_d - L_q\right)\omega_e i_{qT} + \frac{\left(R_s + R_c\right)}{R_c^2}\left(\lambda_m + L_d i_{dT}\right)L_d\omega_e^2 \quad (10)$$

$$Q = R_s i_{qT} + \frac{R_s}{R_c}\left(\lambda_m + \left(L_d - L_q\right)i_{dT}\right)\omega_e + \frac{\omega_e^2}{R_c^2}\left(R_s + R_c\right)L_q^2 i_{qT} \quad (11)$$

By equaling the right hand side of (8) and (9) and rearranging the result, the mentioned condition is obtained as:

$$-\frac{\omega_e^2}{R_c^2}L_d\lambda_m\left(R_s + R_c\right)\left[\lambda_m + \left(2L_d - L_q\right)i_{dT}\right] - R_s\lambda_m i_{dT} + \frac{\omega_e^2}{R_c^2}\left(R_s + R_c\right)\left(L_d - L_q\right)\left(L_q^2 i_{qT}^2 - L_d^2 i_{dT}^2\right) + R_s\left(L_d - L_q\right)\left(i_{qT}^2 - i_{dT}^2\right) = 0 \quad (12)$$

IV. Sliding Mode Controller

In this Section a sliding mode controller is designed to provide both high performance motor drive operation and loss minimization.

A. Coordinate System

In order to control the developed torque and efficiency, the system outputs are chosen as:

$$y_1 = T_e = \frac{3P}{2}\left[\lambda_m + \left(L_d - L_q\right)i_{dT}\right]i_{qT} \quad (13)$$

$$y_2 = -\frac{\omega_e^2}{R_c^2}L_d\lambda_m\left(R_s + R_c\right)\left[\lambda_m + \left(2L_d - L_q\right)i_{dT}\right] - R_s\lambda_m i_{dT} + \frac{\omega_e^2}{R_c^2}\left(R_s + R_c\right)\left(L_d - L_q\right)\left(L_q^2 i_{qT}^2 - L_d^2 i_{dT}^2\right) + R_s\left(L_d - L_q\right)\left(i_{qT}^2 - i_{dT}^2\right) = 0 \quad (14)$$

According to feedback linearization theorem, outputs y_1 and y_2 have to be differentiated successively with respect to time, until one of the components of the control vector $u=(v_d\ \ v_q)^T$ appears [6]. By differentiating (13) and (14) and substituting from (1) and (2), a new coordinate system can be introduced as:

$$\begin{pmatrix}\dot{y}_1\\ \dot{y}_2\end{pmatrix} = \begin{bmatrix}f_1\\ f_2\end{bmatrix} + \begin{bmatrix}g_1 & g_2\\ g_3 & g_4\end{bmatrix}\begin{bmatrix}v_d\\ v_q\end{bmatrix} \quad (15)$$

where f_1 and f_2 and g_1-g_4 are given in Appendix I. Furthermore, using the nonlinear feedback linearization control method to decouple the control inputs, the resulting system is [14]:

$$\begin{pmatrix}\dot{y}_1\\ \dot{y}_2\end{pmatrix} = \begin{bmatrix}f_1\\ f_2\end{bmatrix} + \begin{bmatrix}0 & 1\\ 1 & 0\end{bmatrix}\begin{bmatrix}\hat{v}_d\\ \hat{v}_q\end{bmatrix} \quad (16)$$

and the linear feedback is defined as:

$$\begin{bmatrix}\hat{v}_d\\ \hat{v}_q\end{bmatrix} = \begin{bmatrix}g_3 v_d + g_4 v_q\\ g_1 v_d + g_2 v_q\end{bmatrix} \quad (17)$$

Owing to (16) being a nonlinear system, the dynamics are hard to regulate by a constant state feedback gain [13]. Therefore, for the dynamic system of (16), a model-following nonlinear sliding mode controller is proposed to track a desired reference model. The reference model is designed in a linear form as:

Loss Minimization Sliding Mode Control of IPM Synchronous Motor Drives

Mehran Zamanifar[(1)] - Sadegh Vaez-Zadeh[(2)]
(1) Ph.D Condidate - Department of Electrical Engineering, Isfahan University of Technology, Isfahan
(2) Proffesor - Department of Electrical Engineering, Tehran University, Tehran

Received: Summer 2009 Accepted: Autumn 2009

Abstract: In this paper, a nonlinear loss minimization control strategy for an interior permanent magnet synchronous motor (IPMSM) based on a newly developed sliding mode approach is presented. This control method sets force the speed control of the IPMSM drives and simultaneously ensures the minimization of the losses besides the uncertainties exist in the system such as parameter variations which have undesirable effects on the controller performance except at near nominal conditions. Simulation results are presented to show the effectiveness of the proposed controller.

Index Terms: Permanent magnet motors, speed control, loss minimization control, sliding mode.

I. Introduction

Interior permanent magnet synchronous (IPMS) motors are widely used in high performance drive applications such as robotics, aerospace and electric vehicles (EV) [1,2]. These applications require demanding still practical control methods [4]. Thus much effort has been directed towards the efficiency optimization control (EOC) of the IPMS motors by minimizing machine copper and iron losses [5-8]. Model-based EOC methods are very fast and do not produce torque ripples; but they are not robust against machine parameter variations [5-7]. The stator resistance may vary due to the skin effects, temperature variations, etc. Core losses also vary due to the variations of motor flux and speed and become an important issue at high speeds [8]. Also permanent magnet (PM) flux may vary due to temperature variations and excessive flux weakening. Machine inductance is known to depend on air-gap flux [9]. The adverse effect of motor parameter variations on minimum loss operation of IPMS motors is analyzed in [10,11] and it is shown that these parameter variations except at near nominal conditions have undesirable effects on the controller performance. Thus, it is vital to compensate the variation of the mentioned parameters in the high performance IPMS motor drives especially when an EOC is used.

Sliding mode control (SMC) has been studied by many researchers due to its favorable advantages, such as insensitivity to parameter variations and external load disturbances [12-13]. Only the bounds of the uncertainties are needed. The robustness of this controller is guaranteed, but the worst drawback is the chattering, which limits the applications of SMC. The chattering phenomenon is greatly considered as motion which oscillates about the sliding surface. There are two possible mechanisms which produce such a motion. First, the presence of switching device non-idealities such as delays; second, the presence of parasitic dynamics (actuator and sensor dynamics) in series with the plant. Using a discrete-time control design approach, or high sample rate,we can reduce the chattering due to the switching device non-idealities. Several methods, observer-based sliding mode control, sliding mode based on disturbance compensation and boundary layer sliding mode control have been used to reduce the chattering due to parasitic dynamics. The most common and simplest approach to reduce the effects of chattering has been the boundary layer [14].

In this paper, a newly designed sliding mode controller for an IPMS motor drive is introduced to both minimize the machine losses and track a reference speed command. Finally, extensive simulation results are presented to show robust, efficient and high performance motor drive operation under the proposed control system.

II. Machine Model

Under certain assumptions a widely used model for an IPM synchronous motor including copper and iron losses in a synchronously rotating reference frame is presented in Fig. (1) [5,10]:

The model equations are given as follows:

$$\frac{di_{dT}}{dt} = \frac{R_c}{L_d(R_s+R_c)}\left(-R_s i_{dT} + v_d\right) + \frac{L_q}{L_d}\omega_e i_{qT} \quad (1)$$

$$\frac{di_{qT}}{dt} = \frac{R_c}{L_q(R_s+R_c)}\left(-R_s i_{qT} + v_q\right) - \frac{\omega_e}{L_q}\left(L_d i_{dT} + \lambda_m\right) \quad (2)$$

$$T_e = \frac{3P}{2}\left[\lambda_m + \left(L_d - L_q\right) i_{qT}\right] \quad (3)$$